JAAS

PAPER

View Article Online
View Journal | View Issue

Cite this: J. Anal. At. Spectrom., 2025, 40, 2763

Kinetic analysis of boron therapeutics in head and neck cancer cells by complementary bulk ICP-MS and single-cell (scICP-MS) approaches

Jack G. Finch,†[a] Rhiannon J. Pass, †[a] Maria Rita Fabbrizi, [b] Aimee E. P. McLoughlin, [a] Stuart Green, [c] Jason L. Parsons [b] and James P. C. Coverdale *[ad]

Boron neutron capture therapy (BNCT) is an emerging approach to radiotherapy. Neutron capture by a boronated (^{10}B) therapeutic yields high linear energy transfer alpha particles (helium nuclei, ^{4}He) and lithium-7 (^{7}Li) atoms, eliciting a localised cell kill effect. Current methods to quantify boron in cells either infer from circulatory concentrations and/or often overlook rapid boron pharmacokinetics. By considering both sample preparation requirements and biological boron dynamics, we report two novel approaches to quantify intracellular boron: firstly, rapid *in situ* tryptic and acidic digestion of treated cells to avoid premature B efflux (LOD $^{10}B^{+}$ = 0.2 μg L^{-1}, LOD $^{11}B^{+}$ = 0.4 μg L^{-1}) with method suitability confirmed by pre- and post-digestion spike recoveries (102.5 ± 0.5% and 103 ± 3% recovery, respectively); secondly, real-time measurement of boron in live cells using single-cell ICP-MS (scICP-MS) revealing real-time monitoring of boron efflux: biological half-life of *ca.* 6 min. These complementary approaches deliver unprecedented insight into boron influx and efflux and provide essential bioanalytical tools to advance both BNCT therapeutic development and single-cell elemental analysis.

Received 9th June 2025
Accepted 13th August 2025

DOI: 10.1039/d5ja00228a

rsc.li/jaas

Introduction

Head and neck squamous cell carcinoma (HNSCC) is the 7th most common form of cancer worldwide with incidences of ~890 000 cases per year and ~450 000 deaths per year.[1] X-ray radiotherapy is often used,[2] however *ca.* 40% of patients will develop a recurrence within 5 years,[3] and a significant number of survivors will be at risk of radiation-induced secondary malignancies.[4] Boron neutron capture therapy (BNCT) represents an alternative approach which combines boronated small molecule therapeutics with neutron irradiation to selectively target tumours.[5,6] Upon irradiation, low energy thermal neutrons are captured by ^{10}B, leading to the release of high linear energy transfer (LET) α-particles and lithium-7 (^{7}Li) atoms which are sustained for a combined range of up to 15 microns, causing a localised cell kill effect.[7] Due to the high-LET radiation delivered, BNCT is significantly more biologically effective than conventional radiotherapy.[2,8] Early BNCT studies were conducted using isotopically enriched boric acid, which was not selectively accumulated by tumoral cells compared with surrounding tissues.[9] In response, second generation therapeutics were identified: L-4-dihydroxy-borono-phenylalanine (L-BPA) and sodium borocaptate (BSH) which are currently under clinical evaluation for the treatment of glioblastomas, melanomas, meningiomas, as well as HNSCC.[10,11]

Successful neutron capture is dependent on achieving high boron accumulation in cancer cells. It is generally accepted that viable BNCT requires tumoral boron concentrations of 20–50 μg g^{-1},[12] though successful BNCT has been reported in 22Rv1 prostate xenograft tumours at 4–7 μg g^{-1} boron.[13] In the clinic, tumoral boron accumulation is often inferred from the circulatory boron concentration,[14] but this approximation does not account for differences between tumoral and circulatory clearance.[15] Boron quantitation using ICP-MS is well established, though memory effects (adhesion to sample introduction apparatus) and interference from adjacent $^{12}C^{+}$ (particularly for biological samples) should be considered during method optimisation.[16,17] Reliable measurement of intra-cellular boron presents a further analytical challenge: boric acid and other small molecule boron agents can freely and rapidly diffuse across cell membranes.[18] Despite using a clinically relevant dose of 25–150 μg mL^{-1} boron, ICP-MS quantitation of boric acid treated telomerase immortalized human microvascular endothelial cells and EA.hy926 cells by Verlinden and coworkers did

[a]Department of Pharmacy, School of Heath Sciences, College of Medicine and Health, University of Birmingham, Edgbaston, B15 2TT, UK. E-mail: j.p.coverdale@bham.ac.uk

[b]Department of Cancer and Genomic Sciences, College of Medicine and Health, University of Birmingham, Edgbaston, B15 2TT, UK

[c]Department of Medical Physics, University Hospital Birmingham NHS Trust, Edgbaston, B15 2TH, UK

[d]Department of Chemistry, University of Warwick, Coventry, CV7 7AL, UK

† Jack G. Finch and Rhiannon J. Pass are joint first authors of this manuscript.

not detect intracellular boron above the limit of detection (LOD).[19] Valuable strategies for carbon removal and the suitability of external calibration standardisation were described, but rapid diffusion (efflux) from cells did not appear to be considered as a contributing factor.

An emerging alternative approach to whole-cell (bulk) quantitation is single-cell inductively coupled plasma mass spectrometry (scICP-MS), which facilitates measurement of elements at the single-cell level. The technique remains limited by sample handling challenges, but advances in sample introduction and preparation methodology have increased its application.[20] A common approach is to apply chemical fixation to preserve cells for analysis: calcium and iridium content have been quantified in single cells using 70% ethanol fixation,[21,22] while 4% formaldehyde solution has been employed to measure endogenous elements in HepG2 liver cells,[23] and 2% PFA was used to quantify platinum in single ovarian cancer cells.[24] Organic modifiers (*e.g.* 10% methanol) have also been used in scICP-MS improve nebulisation performance,[25] but will impact cellular fixation. Importantly, chemical fixatives disrupt membrane physiology and permeability, so are unsuitable when examining dynamic systems like those of boron. More recent efforts have explored live cell 'native' analysis (without the addition of chemical fixative) but analytical considerations have often required biological trade-offs. Meyer *et al.* studied arsenite bioavailability in A549 cells using scICP-MS by directly re-suspended cells in water,[26] neglecting hypotonicity and resulting cell turgidity. Buffer solutions have been explored: Galé and coworkers used a phosphate buffered saline/water (1 : 3) mobile phase to quantify platinum uptake (from cisplatin) in single cells,[27] while Shum *et al.* quantified a range of endogenous analytes in sperm cells using a HEPES-buffered medium. Though these approaches address pH, and to a degree osmolarity, non-volatile buffer salts will lead to deposition on interface cones over time.

In this work, we report methodology to achieve single-cell boron quantitation using an MS-compatible ammonium acetate buffer to achieve scICP-MS in live unfixed cells. Ammonium acetate is a volatile buffer that readily decomposes into volatile species (NH_3 and CO_2) during desolvation and ionisation processes. This property is essential for mass spectrometry, where non-volatile salts or buffers (*e.g.* phosphate, Tris, HEPES) would otherwise lead to salt deposition on interface cones. From a theoretical perspective, ammonium acetate is widely recognised as an MS-compatible buffer.[28] Moreover, 100 mM ammonium acetate provides osmolarity nearly equivalent to that of culture medium,[29] maintaining cell morphology and membrane integrity during short-term handling and measurement of live cells. This is essential to ensure elemental quantitation reflects the true intracellular concentration, rather than artefacts from osmolysis or compromised membranes.

Experimental

Materials and methods

Ammonium acetate (99.9999% trace metal basis), ammonium hydroxide (99.9999% trace metal basis), cisplatin, nitric acid (72%, 99.9999% trace metal basis), trichloroacetic acid, sulforhodamine B dye, and Tris base were purchased from Merck (UK). All cell culture reagents (DMEM, MEM, non-essential amino acid solution, foetal calf serum, trypsin/EDTA (0.25%) solution, penicillin/streptomycin solution (10 000 units), and Dulbecco's phosphate buffered saline, (D-PBS) were purchased from Merck (UK). L-BPA (97%) was purchased from Fisher Scientific (UK). Inorganic Ventures certified reference materials for boron (1000 mg L^{-1} natural abundance B from H_3BO_3 in water with trace ammonium acetate) and zinc (1000 mg L^{-1} natural abundance Zn from Zn metal in 2% v/v nitric acid) were purchased from Essex Scientific Laboratory Supplies (UK). Certified reference material for germanium (1000 mg L^{-1}) was purchased from Merck. EQ four element calibration beads were purchased from Standard BioTools (USA). Sterile plasticware was purchased from Scientific Laboratory Supplies (UK) and Starlab (UK). Anti-LAT1 primary antibody was purchased from Cell Signalling Technology (USA). Odyssey blocking buffer was purchased from Li-COR Biosciences (UK). Immobilon FL PVDF membranes were purchased from Millipore (UK). Anti-actin primary antibody was purchased from Merck (UK).

Cell culture

UM-SCC-74A cells (kindly provided by Professor Thomas Carey, University of Michigan, USA) were maintained in Dulbecco's Modified Eagle's Medium (DMEM) supplemented with foetal calf serum (10% v/v), penicillin/streptomycin (1% v/v) and MEM non-essential amino acid solution (1% v/v). FaDu cells (acquired from ATCC, Virginia, USA) were maintained in Minimum Essential Medium (MEM) supplemented with foetal calf serum (10% v/v), penicillin/streptomycin (1% v/v) and MEM non-essential amino acid solution (1% v/v). Cells were passaged at twice weekly intervals using trypsin/EDTA, used at low passage number, and maintained in a 5% CO_2 humidified environment at 37 °C (standard conditions).

Antiproliferative activity (GI_{50}) determination

Half-maximal growth inhibition concentrations (GI_{50}) were determined using the sulforhodamine B (SRB) assay. Briefly, 5×10^4 UM-SCC-74A or FaDu cells were seeded in 96-well plates and incubated under standard conditions for 48 h. The supernatant was removed by aspiration, and cells were treated with defined concentrations of boric acid (0.0001–50 mM) prepared by serial dilution of a 1000 mg L^{-1} boric acid certified reference material (H_3BO_3 in water, sterilised by 0.2 μm filtration) or L-BPA prepared as a stock solution in 10% w/v mannitol (Merck), sterilised using a 0.2 μm sterile filtration, and the stock concentration standardised by ICP-MS before use. Cells were incubated for 24 h exposure time. The supernatant was then removed by aspiration, cells were washed with D-PBS (100 μL) and to each well was added ice-cold 10% v/v trichloroacetic acid solution for 1 h. Fixed cells were washed with water using a Molecular Devices Multiwash+ microplate washer, and excess water was removed by blotting onto paper towel. To each well was then added 50 μL sulforhodamine B (0.4% v/v dye in 1% v/v acetic acid) for 30 min. Excess dye was removed by sequential

washes with 1% acetic acid using a Molecular Devices Multiwash+ microplate washer and blotting onto paper towel. Tris base (10 mM, pH 10, 200 μL) was added to each well and incubated for 1 h. Absorbance (492 nm) was measured using a BMG Labtech FLUOstar Omega microplate reader. Data were analysed using Microsoft Excel and GraphPad Prism 10 for MacOS, to calculate half-maximal growth inhibition concentrations (GI_{50}) from dose–response fitting. Calculated values were reported as the mean ± standard deviation of two independent biological experiments, each performed in experimental triplicate (duplicate of triplicate analysis).

ICP-MS sample preparation: acidic digestion

All cellular accumulation experiments were performed in biological triplicate. Briefly, 5×10^5 UM-SCC-74A or FaDu cells were seeded in P100 dishes and incubated under standard conditions for 24 h. The supernatant was removed by aspiration, and cells were treated with a fixed concentration of boric acid (4.63 mM, 10 mL, 50 mg L^{-1} boron equivalent) for 0–24 h with or without recovery time in boron-free medium ± phenylalanine supplementation (4.63 mM, 10 mL). After this time, the supernatant was removed by aspiration, cells were washed D-PBS and harvested with trypsin/EDTA (1 mL). Trypsin activity was quenched by addition of a known volume of cell culture medium (typically 6 mL) and a cell count obtained in duplicate per sample (10 μL using a C-Chip disposable haemocytometer). A cell pellet was obtained by centrifugation (1000 rpm, 5 min) which was further washed with D-PBS (1 mL), transferred to an Eppendorf, and the supernatant removed by centrifugation (1000 rpm, 5 min). Pellets were digested by addition of 72% v/v ultrapure nitric acid (200 μL, 50 °C, overnight) and subsequently diluted to a 3.6% v/v working acid concentration using type I water. Spike-recovery experiments ($N = 5$) were prepared by standard addition of certified reference material to achieve a final working concentration of 50 mg L^{-1} boron, either prior to, or post-digestion.

ICP-MS sample preparation: *in situ* digestion

This experiment was carried out as described for acidic digestion with the following modifications: cell counts were obtained in duplicate per sample, from a set of triplicate biological samples. After removal of the boron-containing supernatant by aspiration, cells were washed with D-PBS (2 × 20 mL) and subject to *in situ* tryptic digestion (0.25% trypsin in ammonium acetate, 99.9999% trace metal basis, 100 mM, pH 7.4 adjusted using trace metal grade ammonium hydroxide) at 37 °C. Once cell detachment was observed (*ca.* 5 min) cells were mixed by pipetting to achieve a single cell solution, from which a cell count (10 μL using a C-Chip disposable haemocytometer) was determined. To further exploit protease action, cells were maintained in trypsin for 24 h. To each sample was then added 72% v/v ultrapure nitric acid (50 °C, overnight) and then samples were diluted to achieve a working acid concentration of 3.6% v/v using type I water.

Single-cell scICP-MS sample preparation

Single-cell samples for scICP-MS analysis were prepared immediately prior to analysis: UM-SCC-74A cells were treated with boric acid (4.63 mM, 50 mg L^{-1} boron equivalent) for 2 h and harvested using trypsin/EDTA. Trypsin activity was quenched by the addition of cell culture medium, a cell pellet was obtained by centrifugation (2000 rpm, 1 min) and the supernatant medium was removed by aspiration. Cells were then washed with D-PBS and the supernatant removed by centrifugation (1000 rpm, 5 min). Cells were re-suspended in ammonium acetate buffer (99.9999% trace metal basis, 100 mM, pH 7.4 adjusted using trace metal grade ammonium hydroxide) in preparation for scICP-MS.

ICP-MS analysis

Acid digest samples were analysed using a NexION 300X inductively coupled plasma mass spectrometer (ICP-MS) fitted with a PerkinElmer S10 autosampler, low-adsorption PFA nebuliser and spray chamber. To minimise boron memory effects, extended rinse time (3.6% v/v HNO_3) was included between all samples and standards. Nebulizer gas flow: 0.94 L min^{-1}, auxiliary gas flow: 1.2 L min^{-1}, plasma gas flow: 18.0 L min^{-1}, ICP RF power: 1600 W. Multi-element calibrants (B and Zn, 0.1–1000 μg L^{-1}) were freshly prepared in 3.6% v/v ultrapure nitric acid from single-element certified reference materials. Limits of detection (LOD, 3σ) and quantification (LOQ, 10σ) were calculated for each analyte from sample blank replicates ($N = 10$). Data for $^{10}B^+$ and $^{11}B^+$ (no-gas mode) and $^{66}Zn^+$ (He-gas mode) were acquired using Syngistix (version 3.3) for Windows (PerkinElmer Inc.) and processed using Microsoft Excel. Boron and zinc concentrations were normalised by cell number. Statistical analyses were calculated at the 95% confidence level using a two-tailed *t*-test assuming unequal sample variance (Welch's *t*-test).

Immunoblotting

Whole cell extracts were prepared from the cell pellets as previously described.[30] Protein extracts (40 μg) were separated by 10% Tris-glycine SDS-PAGE then proteins were transferred onto an Immobilon FL PVDF membrane. Membranes were blocked using Odyssey blocking buffer and incubated with the anti-LAT1 primary antibody overnight at 4 °C or with the anti-actin primary antibody at room temperature for 1 h. Membranes were washed with PBS containing 0.1% Tween-20, incubated with either Alexa Fluor 680 or IR Dye 800 secondary antibodies at room temperature for 1 h, then further washed with PBS containing 0.1% Tween 20. Proteins were visualized and quantified using a Li-COR Biosciences Odyssey image analysis system.

Single-cell scICP-MS analysis

Single-cell ICP-MS samples were analysed using a NexION 300D inductively coupled plasma mass spectrometer (ICP-MS) fitted with an Elemental Scientific MicroFAST MC autosampler for single-cell analysis, an Asperon spray chamber and a high-

efficiency nebuliser (HEN). Flow rate: 0.01 mL min^{-1}, dwell time: 40 μs, scan time: 40 s, nebuliser gas flow: 0.4 L min^{-1}, makeup gas flow: 0.7 L min^{-1}, auxiliary gas flow: 1.2 L min^{-1}, plasma gas flow: 18 L min^{-1}, ICP RF power: 1600 W. Data $^{11}B^+$ or $^{165}Ho^+$ (no-gas mode) were acquired in time-resolved analysis (single-cell mode) using Syngistix (version 3.3). Transport efficiency was determined using EQ rare-earth element doped cytometry calibration beads containing $^{131/133}Eu$, $^{135/136}Lu$, $^{140/142}Ce$ and ^{165}Ho prepared at a density of 3.3×10^4 particles per mL in ammonium acetate (99.9999% trace metal basis, 100 mM, pH 7.4 adjusted using trace metal grade ammonium hydroxide). Boron calibration standards (0.1–1000 μg L^{-1}) were freshly prepared in ammonium acetate (99.9999% trace metal basis, 100 mM, pH 7.4) from a single-element certified reference material. Data were acquired and processed using Syngistix (version 3.3) for Windows (PerkinElmer Inc.), with post-processing in Microsoft Excel and GraphPad Prism 10 for MacOS. The mass of analyte (^{11}B) per cell (m, ag per cell) was calculated as the product of transport efficiency (η), sample flow rate (Q_s), dwell time (t_d) and the background-corrected signal ($I_{sample} - I_{background}$) divided by the gradient of the calibration (b). Single-cell analysis was performed in a time-dependent manner ($t = 9 \pm 1$ min, 17 ± 1 min, 26 ± 1 min and 41 ± 1 min) where t_0 is defined as the time the boron-containing supernatant was removed. Single cell events were characterised as peaks defined by a minimum of five sequential measurements (*i.e.* 5×40 μs, exemplar data shown in Fig. 3 and SI). Data were reported as a histogram of boron mass per cell (^{11}B, ag per cell, bin width = 400) and a Gaussian distribution fitted using a non-linear regression model (Prism 10). Mean ^{11}B content was plotted as a function of time and fitted using a one-phase decay model to determine biological half-life.

Statistical analysis

All experimental data are reported as the mean ± standard deviation. Statistical significance was determined using an unpaired, two-tailed *t*-test assuming unequal sample variances (Welch's *t*-test) at the 95% confidence level ($p < 0.05$).

Results and discussion

Acidic (bulk) digestion method development

Growth inhibition (GI_{50}) by boric acid was initially determined using the sulforhodamine B assay in two HNSCC models: $GI_{50} = 30 \pm 1$ mM in UM-SCC-74A cells, 32 ± 6 mM in FaDu cells (Fig. 1a and SI Table S1), confirming that cellular accumulation experiments could be undertaken using a dose that is both clinically relevant (typically administered to achieve 50 mg L^{-1} intracellular boron) and non-lethal to cells in 2D adherent culture.[12] With this knowledge in hand, boron accumulation was quantified in cells using inductively coupled plasma mass spectrometry (ICP-MS). Although ^{11}B has greater natural abundance (0.801(7) natural abundance), samples containing high levels of organic carbon (^{12}C) may impact $^{11}B^+$ quantitation, and the ^{10}B isotope (0.199(7) natural abundance) is essential for BNCT. Zinc (as $^{66}Zn^+$) was also quantified as a proxy for cell content. Limits of detection (LOD, 3σ) were determined for each analyte from ten sample blank replicates: $^{10}B^+ = 0.2$ μg L^{-1}, $^{11}B^+ = 0.4$ μg L^{-1}, $^{66}Zn^+ = 0.8$ μg L^{-1}. Spike-recovery experiments (50 mg L^{-1} B) pre- and post-digestion (72% v/v HNO_3, 50 °C, overnight) revealed no significant impact of acidic digestion on boron spike recovery ($102.5 \pm 0.5\%$ and $103 \pm 3\%$ respectively). Furthermore, no $^{10}B^+$ or $^{11}B^+$ was measured above LOD in unspiked cell pellets ($1–5 \times 10^6$ cells) after acidic digestion, relative to the cell-free external calibrants (SI, Table S2), excluding significant interference (*e.g.* from $^{12}C^+$) under these conditions.

With analytical methodology in hand, cells were treated with a range of concentrations of boric acid (0.001–10 mM) for 24 h. Initially, after acidic digestion of cell pellets, no boron was detected above the limit of detection (SI, Table S2), consistent with previous efforts.[19] To exclude exposure time (*e.g.* slow uptake or rapid efflux) the experiment was repeated with time-dependent exposure to an equimolar treatment of boric acid (50 mg L^{-1} boron equivalent) yet still, no boron was detectable (SI, Table S3). This result was surprising, given the high treatment concentration and apparent analytical sensitivity. During these initial experiments, cells were harvested using trypsin/EDTA and cell pellets obtained by re-suspension and centrifugation, the complete biological sample preparation requiring up to 1 h per sample. However, boric acid diffusion across membranes is rapid: the permeability coefficient of boric acid in *Xenopus* oocytes is 1.5×10^{-6} cm s^{-1},[31] while in phosphatidylcholine liposomes, boric acid permeability coefficients ranged from 7×10^{-6} to 9.5×10^{-9} cm s^{-1} depending on the presence of sterols, the type of phospholipid head group, the length of the fatty acyl chain, and pH.[32]

It was hypothesised that intracellular boron rapidly effluxes into the supernatant during biological sample collection and processing. In response, we revised our sample preparation methodology to minimise the time between removal of the supernatant and elemental analysis. Immediately after treatment of adherent cells with boric acid, cells were washed with excess phosphate buffered saline (2×20 mL) and digested *in situ* by addition of 0.25% trypsin in ammonium acetate (99.9999% trace metal basis, 100 mM) for 24 h followed by ultrapure nitric acid (72% v/v, 50 °C) for a further 24 h, before diluting to a working nitric acid concentration of 3.6% v/v. The trypsin incubation time was intentionally extended (24 h, compared to conventional trypsinisation of *ca.* 5 min) to exploit protease action for both detachment from the culture surface and initial cell digestion. This reduced sample handling time (*i.e.* from removal of boron-containing medium to addition of trypsin solution which remains in the final sample) from minutes to seconds, enabling quantification of analytes with moderately rapid flux. Both isotopes of boron (^{10}B and ^{11}B) were measured in all samples to exclude significant interference from organic (cell-derived or ammonium acetate) neighbouring $^{12}C^+$. No significant difference between $m/z = 10$ and $m/z = 11$ was observed (see SI for full ICP-MS data).

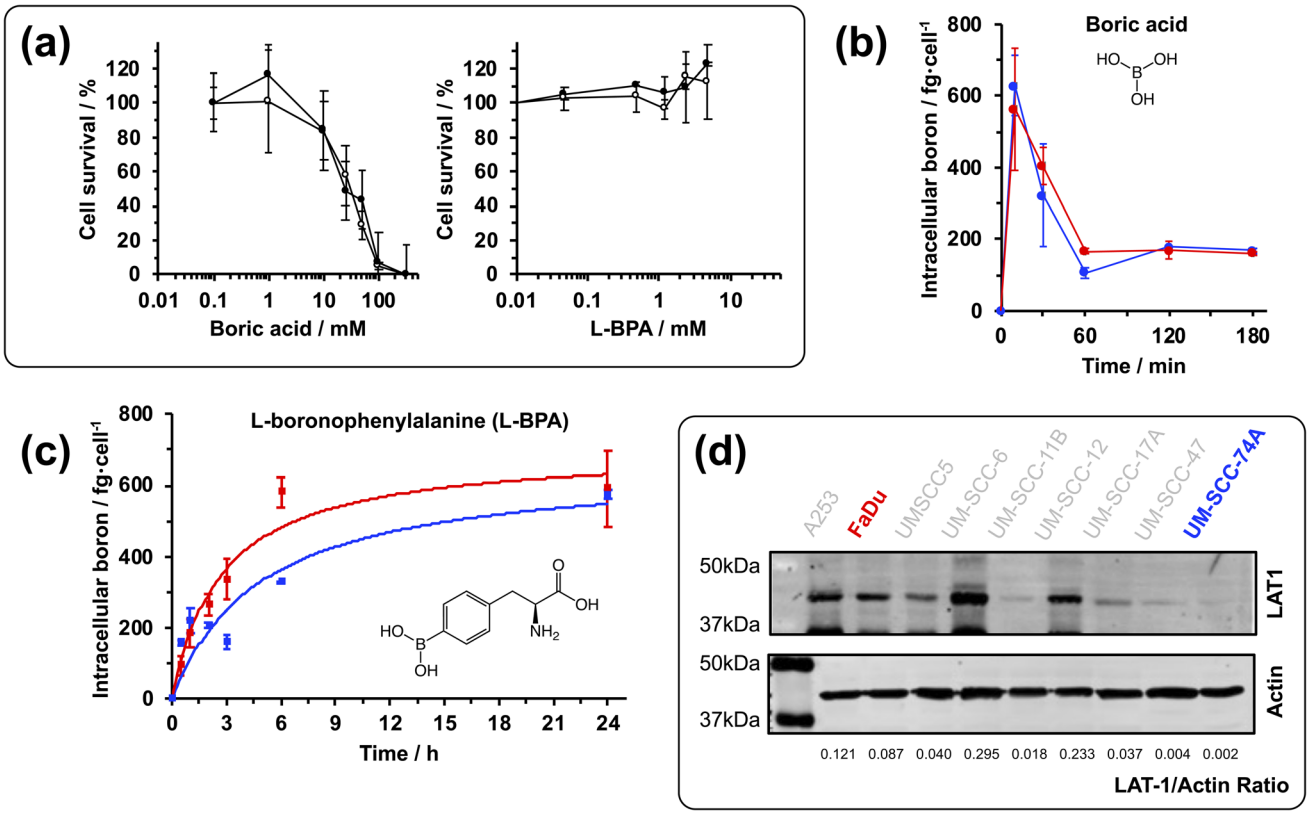

Fig. 1 Biological cytotoxicity and cellular accumulation of boron in cancer cells. (a) GI_{50} determination (24 h) for boric acid or L-BPA in UM-SCC-74A cells using the SRB assay. Cell viability experiments were determined as part of two independent biological experiments; each performed in triplicate. (b) Intracellular boron (fg per cell) determined in UM-SCC-74A (blue) or FaDu (red) cells treated with equimolar concentrations (4.63 mM, 50 mg L^{-1} boron equivalent) of boric acid. (c) Intracellular boron (fg per cell) determined in UM-SCC-74A (blue) or FaDu (red) cells treated with equimolar concentrations (4.63 mM, 50 mg L^{-1} boron equivalent) of L-BPA. Non-linear curve fits used a Michaelis–Menten derived non-linear regression: K_m(UM-SCC-74A) = 4.896 h, K_m(FaDu) = 2.758 h, V_{max}(UM-SCC-74A) = 660.1 fg per cell, V_{max}(FaDu) = 703.5 fg per cell. Fitting constraint: $K_m > 0$. Accumulation data are the average of three independent biological samples ($N = 3$). All error bars are ±standard deviation. Full numerical data can be found in the SI. (d) LAT1 and actin immunoblotting in a panel of head and neck squamous cell carcinoma (HNSCC) lines, reported with LAT1/actin ratios. Full uncropped gels are found in the SI.

In situ digestion analysis

Time-dependent sampling was repeated using this revised sample preparation, revealing rapid boron accumulation in both UM-SCC-74A and FaDu cell lines treated with 4.63 mM boric acid (50 mg L^{-1} boron equivalent) reaching an intracellular concentration of 629 ± 82 fg per cell for UM-SCC-74A and 563 ± 171 fg per cell for FaDu within 30 min. Equimolar treatment resulted in statistically similar accumulation profiles, irrespective of the HNSCC cell line. Within *ca.* 1 h, boron accumulation in both cell lines reduced to a linear plateau (*ca.* 160–180 fg per cell) which was sustained for the remaining duration, establishing an equilibrium with the extracellular medium concentration. Assuming the volume of a FaDu cell to be 3 ng,[33] 160 fg per cell is equivalent to *ca.* 50 mg L^{-1} intracellular boron, *i.e.* equilibrium established with extracellular concentration (Fig. 1b). Using atomic emission spectroscopy (ICP-AES) after microwave digestion of cells treated with 65% HNO_3/30% H_2O_2, Huang *et al.* quantified 60–80 fg per cell intracellular boron in HepG2 cells treated with 25 mg L^{-1} boric acid, and identified a similar linear plateau from 0.5–2 h.[34]

Though broadly in agreement with our findings (factoring for the lower dosage of boric acid), cell harvesting and digestion appeared to be carried out *ex situ*, although some experimental details are not provided (*e.g.* harvesting method, sample preparation time). In our new approach, *in situ* pellet collection minimises sample preparation time, which may otherwise underestimate the true intracellular concentration. A different study described the harvesting of boric acid treated cells by scraping and low-speed centrifugation (200 rcf, 10 min), determining a boron intracellular concentration of 10–12 μg g^{-1} though curiously, the cell pellet and supernatant were recombined prior to boron quantification.[35] Data comparability is limited by normalisation method (by cell count or mass) and treatment concentration (25 or 50 mg L^{-1} boric acid) but estimation of our data in w/w units (assuming the density of a cell to be 1 g L^{-1}) gives 53–60 μg g^{-1}.[33] Although analyte loss during *ex situ* sample preparation could explain this discrepancy, differing experimental conditions limit the certainty of this interpretation.

Experiments were repeated using the second generation BNCT therapeutic, L-BPA. Similarly to boric acid, L-BPA is non-

toxic to cells at millimolar concentrations (Fig. 1a) and so was administered at an equimolar concentration (4.63 mM, 50 mg L^{-1} boron equivalent). Boron accumulation from L-BPA was slower than that of boric acid and gradually accumulated over 24 h, modelled using Michaelis–Menten derived non-linear regression: K_m(UM-SCC-74A) = 4.896 h, K_m(FaDu) = 2.758 h with similar V_{max} (660.1 and 703.5 fg per cell for UM-SCC-74A and FaDu, respectively) suggesting boron influx was more rapid in FaDu cells but essentially equal to UM-SCC-74A after 24 h treatment (Fig. 1c and SI). Differential rates of L-BPA uptake may be explained by relative expression of the L-type amino acid transporter LAT1 which has previously been associated with L-BPA uptake, particularly at lower L-BPA concentrations.[15,36] Immunoblotting showed LAT1 expression was *ca.* 37-fold greater in FaDu compared with UM-SCC-74A (Fig. 1d). Nonetheless, LAT2 has also been shown to transport L-BPA *in vitro*,[37] while the secondary-active amino acid transporter $ATB^{0,+}$ is thought to contribute to L-BPA uptake at higher concentrations.[36]

Effect of recovery time on boron accumulation

Following 24 h L-BPA treatment, intracellular boron was next measured in cells that had been allowed recovery time in L-BPA-free medium. In contrast to the differential uptake of L-BPA rate during the first 24 h, boron efflux was rapid in both cell lines, and essentially complete (below LOD) within *ca.* 3 h (Fig. 2a). Modelling using a one-phase exponential decay revealed boron efflux to be *ca.* 3-fold faster from FaDu cells than UM-SCC-74A cells (biological half-life, $t_{\frac{1}{2}} = 0.18 \pm 0.05$ h and 0.54 ± 0.04 h respectively, $p = 0.0111$). Hypothesising that rapid efflux may be driven by an amino acid concentration gradient (established after removal of extracellular L-BPA), FaDu cells treated with L-BPA for 24 h were allowed recovery time in medium supplemented with phenylalanine (4.63 mM) which is structurally similar to L-BPA (Fig. 2b). The presence of phenylalanine was hypothesised to saturate amino acid transporters (such as LAT1, for which L-BPA is a known substrate) and thus expected to reduce the rate of L-BPA efflux. Curiously, no significant difference in efflux rate was observed (biological half-life, $t_{\frac{1}{2}} = 0.14 \pm 0.03$ h, $p = 0.5420$). These results at first appear contradictory: FaDu cells (high LAT-1 expression) showed faster L-BPA efflux than from UM-SCC-74A cells, yet medium supplementation with phenylalanine (a LAT-1 substrate) did not impact efflux from LAT-1 expressing FaDu cells. However, only LAT-1 expression was quantified in this work, and while it is likely that various ABC (ATP-binding cassette) or SLC (solute carrier) transporters contribute to L-BPA efflux, such an investigation is beyond the scope of this study.

Single-cell scICP-MS method development

Next, we developed methodology to measure boron in live cells using single-cell ICP-MS (scICP-MS). This emerging technique enables the study of sample heterogeneity at the single-cell level. Our approach was defined by three criteria: (1) analysis of live, viable cells without fixation (alcohol, glutaraldehyde, or other fixatives) that could impact membrane diffusion; (2) identification of an MS-compatible mobile phase that could sustain viable cells for at least 1 h; (3) rapid sample preparation to enable observation of boron in cells. Tris-glucose and D-PBS buffers have been investigated for various bioinorganic

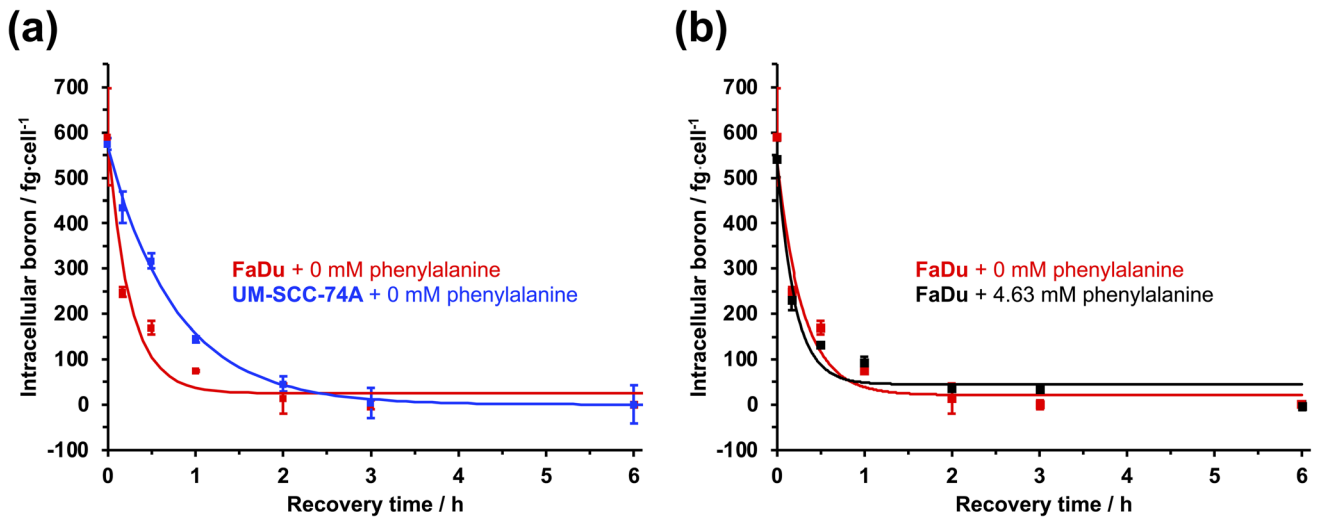

Fig. 2 (a) Intracellular boron (fg per cell) determined in UM-SCC-74A (blue) or FaDu (red) cells treated with equimolar concentrations of L-BPA (4.63 mM, 50 mg L^{-1} boron equivalent) for 24 h, washed with PBS and then allowed recovery time (t = 0–6 h) in L-BPA-free medium. (b) Intracellular boron (fg per cell) determined in FaDu cells treated with equimolar concentrations of L-BPA (4.63 mM, 50 mg L^{-1} boron equivalent) for 24 h, washed with PBS and then allowed recovery time (t = 0–6 h) in either: (i) L-BPA-free medium (red) or (ii) L-BPA-free medium supplemented with equimolar (4.63 mM) phenylalanine (black). Non-linear curve fits used a one-phase exponential decay non-linear regression model: m_0 (intracellular boron at t = 0 h/fg per cell) = 568.0 (FaDu), 532.0 (FaDu + Phe), 566.3 (UM-SCC-74A); m_∞ (intracellular boron at infinite time/fg per cell) = 25.23 (FaDu), 44.99 (FaDu + Phe), 6.375×10^{-6} (UM-SCC-74A); k (rate constant/h^{-1}) = 3.841 (FaDu), 4.866 (FaDu + Phe), 1.284 (UM-SCC-74A). Fitting constraint: $m_\infty > 0$, $k > 0$. Accumulation data are the average of three independent biological samples (N = 3). All error bars are ±standard deviation. Full numerical data can be found in SI Tables S7 and S8.

chemistry applications,[29] but are unsuitable for mass spectrometry due to their non-volatility, leading to salt deposits at the MS interface. In contrast, ammonium acetate has been used to preserve cellular elemental content prior to synchrotron-based X-ray fluorescence microscopy and is widely used for electrospray ionisation mass spectrometry since it can undergo proton transfer to form volatile ammonia and acetic acid.[28] Importantly, ammonium acetate solutions exhibit osmolarity comparable to cell culture medium. Percentage transport efficiency (TE) of particles to the MS source was determined using a counting-based method, *i.e.* the number of single-cell events detected by the instrument relative to a known density of ^{165}Ho-doped cytometry beads as a model of cells. Unlike dissolved (liquid) calibrants which have a constant number of events per dwell time (typically counts per second), single-particle events were defined by a minimum of five sequential data points (40 μs dwell times) to distinguish from background noise (Fig. 3 and SI). TE was determined at the beginning of the batch (and assumed constant) using a well-defined cytometry bead standard containing a known and homogenous metal loading and particle density. This approach was considered preferable to estimation using endogenous cellular elements such as Zn, Fe or Cu, whose inherently heterogeneous intracellular concentrations could obscure the true TE of the system. Using a high efficiency nebuliser and Asperon spray chamber, TE = 25.9% was achieved, in line with similar efforts reported in the literature (8–30%).[38] While examples have reported TE ∼ 100% by including a sheath fluid of PBS to protect the cell suspension,[39] such a high salt matrix is detrimental for repeat or long-term analyses for the aforementioned reasons.

Boric acid was selected as a suitable treatment for scICP-MS method development because it is a membrane-permeable small molecule that is known to rapidly equilibrate across the plasma membrane, leading to relatively homogenous and predictable intracellular boron distribution. This homogeneity is advantageous when establishing and validating scICP-MS and helps to distinguish analytical variability from true biological heterogeneity. L-BPA was shown to be a substrate of LAT-1 (Fig. 2a) so may experience saturation effects, and its accumulation is dependent on LAT1 expression, membrane potential and cellular metabolic state. At this stage, performing scICP-MS on L-BPA treated cells would therefore introduce additional biological variability that could obscure analytical performance. To achieve scICP-MS analysis of boron in live cells, UM-SCC-74A cells were treated with 50 mg L^{-1} boric acid for 2 h, washed with D-PBS to remove extracellular or weakly surface-bound boron, harvested using trypsin/EDTA and immediately resuspended in ammonium acetate, a procedure that could be completed in under 10 min. A low flow rate (10 μL min^{-1}) was used to reduce shear forces and minimise cell lysis prior to (or during) nebulisation, and to further reduce potential misclassification of cell fragments as single cells, we applied post-acquisition filtering based on event duration (a minimum of five sequential measurements) and intensity thresholds. Importantly, the frequency and shape of individual events were symmetric (Fig. S4–S7) which are consistent with intact single cells. Samples were prepared at four efflux timepoints, defined as the time interval after removal of the boric acid-containing supernatant (recovery time). Live-cell autosampling used cell-repellent 96-well plates.

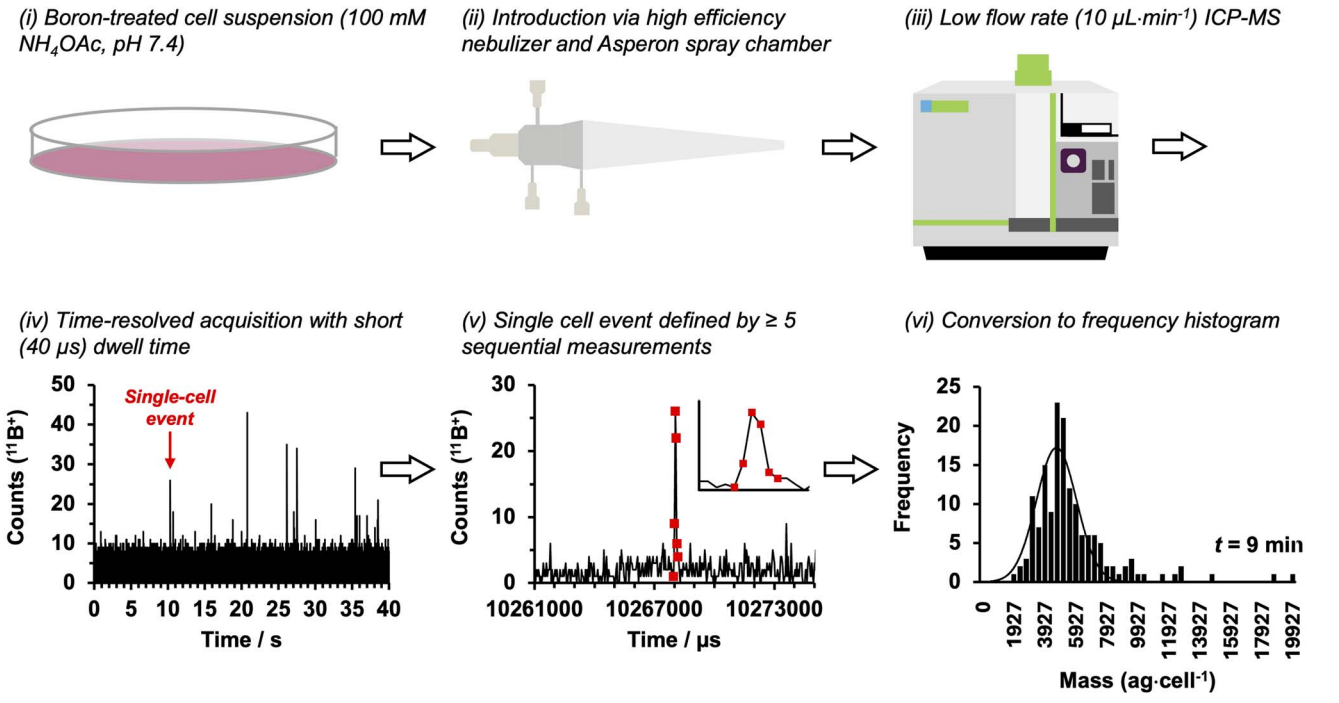

Fig. 3 Schematic single-cell ICP-MS (scICP-MS) workflow: (i) boron-treated cell suspension (100 mM ammonium acetate, pH 7.4); (ii) sample introduction *via* high efficiency nebulizer and Asperon spray chamber; (iii) low flow rate (10 μL min^{-1}) ICP-MS analysis; (iv) time-resolved acquisition with short (40 μs) dwell time; (v) single cell event defined by ≥5 sequential measurements, (vi) conversion to frequency histogram.

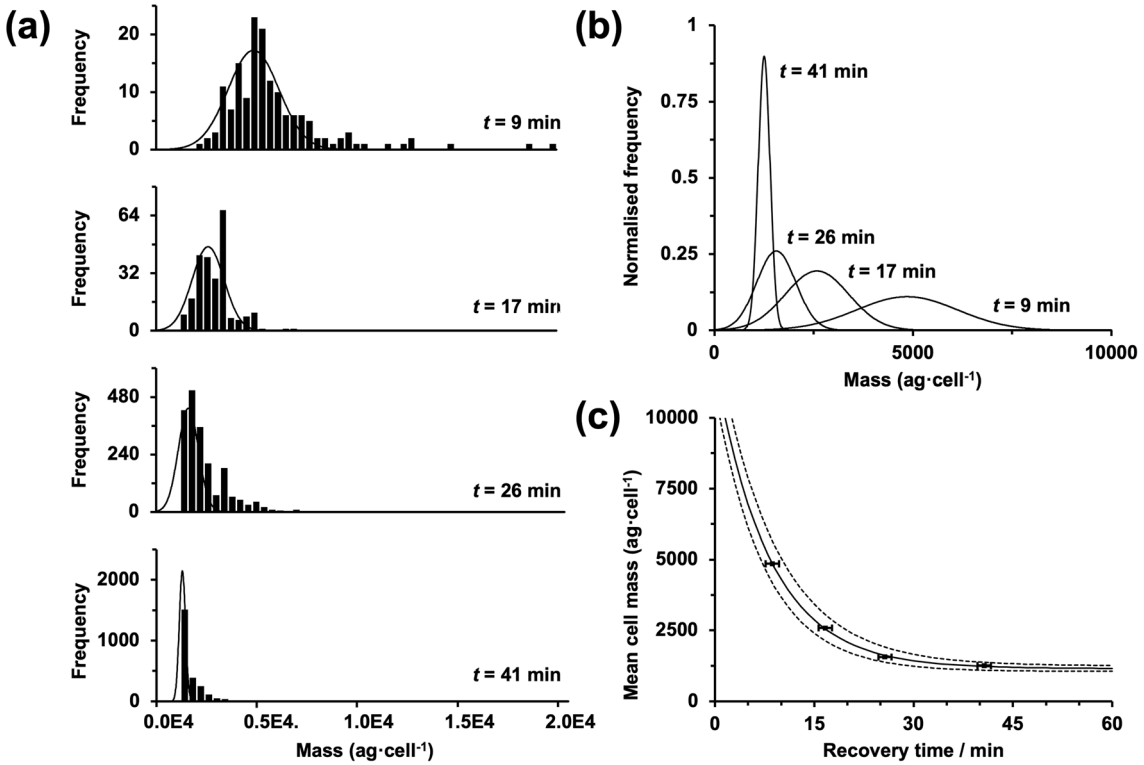

Fig. 4 Intracellular boron efflux (fg per cell) determined in UM-SCC-74A by single-cell ICP-MS (scICP-MS). After 3 h exposure to boric acid (4.63 mM, 50 mg L^{-1} boron equivalent) cells were washed twice with D-PBS (2 × 20 mL) and re-suspended in boron-free medium for variable recovery time (9, 17, 26, 41 min). (a) Frequency histograms (boron mass per cell) were recorded at four timepoints. (b) Normalised frequency histograms. (c) Mean mass as a function of recovery time. Biological half-life (solid line) was modelled using a one-phase exponential decay model (dashed lines show 95% confidence intervals).

As recovery time increased, the intracellular concentration decreased, from 4853 ag per cell ($t = 9$ min) to 1252 ag per cell ($t = 41$ min) (Fig. 4a). Importantly, the mass distribution width narrowed over time, and tended towards a singular theoretical mass per cell (Fig. 4b). This observation was consistent with the experimental design: intracellular boron effluxes into a finite volume of ammonium acetate mobile phase eluent. It was hypothesised that the apparent intracellular concentration at $t = 41$ min is indicative of equilibrium establishment, whereby [intracellular ^{11}B] = [extracellular ^{11}B], since quantification of boron at time t only provides a measure of overall accumulation (*i.e.* competing influx and efflux processes).

One-phase exponential decay modelling of the mean intracellular boron concentration over time ($R^2 = 0.9993$) facilitated measurement of biological half-life, $t_{\frac{1}{2}} = 5.7$ min, 95% CI [1.3, 20.8] (Fig. 4c). This estimation in fact explains our initial experiments which failed to quantify intracellular boron by conventional cell pellet preparation, typically requiring 1 h of sample preparation time. In a worked example calculation, after 1 h (given $t_{\frac{1}{2}}$ *ca.* 6 min), a 160–180 fg per cell intracellular concentration would be reduced to 0.156–0.176 fg per cell (10 biological half-lives). Assuming typical digestion methodology (200 μL of 72% v/v concentrated nitric acid and 20-fold acid dilution to an instrument-compatible working concentration), a typical sample of 1×10^6 cells per 4 mL would have a dissolved concentration of 0.039–0.044 μg L^{-1} after 1 h, an order of magnitude below the limit of detection (^{11}B LOD = 0.4 μg L^{-1}). This worked example was supported by a practical determination: cells were treated with boric acid for 2 h, washed with D-PBS and allowed 1 h recovery time in boron-free cell culture medium (efflux time). Subsequent *in situ* analysis of cells allowed recovery time contained no detectable boron (^{11}B < LOD). Importantly, scICP-MS negates sample dilution requirements of acidic digestion and rapid sample preparation facilitates immediate quantitation of intracellular boron, which in turn enables reliable measurement at later time points (*e.g.* during efflux) when analyte concentration would be too low to detect accurately in bulk digests. Beyond analytical sensitivity, scICP-MS provides biological insights that bulk measurements cannot: boron content is quantified in living cells, allowing observation of cell-to-cell heterogeneity in boron uptake and retention that is discarded by population-averaged bulk analysis. Critically, because scICP-MS preserves cells in a viable state immediately prior to measurement, it permits real-time monitoring of dynamic processes such as boron efflux from cells; an important parameter in understanding intracellular retention and therapeutic efficacy for BNCT. Nonetheless, bulk ICP-MS remains a powerful complementary approach, particularly when combined with *in situ* digestion sample preparation developed in this work, capturing an immediate "snapshot" of total boron content at defined time points, which is especially valuable for rapidly diffusing analytes. Integration of both bulk

analysis and scICP-MS therefore provides a more complete and mechanistically informative overview of boron dynamics.

Conclusions

An 'ideal' compound for BNCT should selectively accumulate in cancerous tumours over healthy tissues, so robust methods to reliably measure boron levels in cells are required to identify next generation boronated drugs. To the best of our knowledge, this is the first example of boron quantitation using single-cell ICP-MS (scICP-MS) and has been applied to quantify boron flux in living cells. This approach provides direct measurement without significantly altering the physiology of the biological sample during analytical preparation, particularly by avoiding use of chemical fixatives that affect membrane permeation. In this application, our findings challenge the existing paradigm which suggested boric acid does not accumulate in cells at concentrations sufficient to overcome ICP-MS limits of detection.[19] By carefully considering both biological sample preparation and analytical instrumentation requirements, boric acid and L-BPA are shown to be rapidly excreted from cells in 2D culture, a finding that may have significant implications on the clinical use of boric acid or L-BPA for BNCT, considering the timing of therapeutic administration and neutron irradiation. Importantly, this analytical toolkit now provides a platform for follow-up pharmacokinetic and pharmacodynamic studies to explore boron flux and dynamics in more complex *in vitro* (*e.g.* spheroid or organoid) and *in vivo* models.

Author contributions

Investigation and formal analysis (J. G. F., R. J. P., M. R. F., A. E. P. M. and J. P. C. C.), conceptualization (S. G., J. L. P. and J. P. C. C.), funding acquisition and supervision (J. P. C. C.). All authors contributed to the review & editing of the manuscript.

Conflicts of interest

There are no conflicts to declare.

Data availability

The data supporting this article have been included as part of the SI. See DOI: **https://doi.org/10.1039/d5ja00228a**.

Acknowledgements

The authors thank the Rosetrees Trust (grant 2024\100198 for J. P. C.) and the Royal Society of Chemistry for Undergraduate Research Bursary (U24-4422287807 for A. E. P. M.).

References

1 M. Gormley, G. Creaney, A. Schache, K. Ingarfield and D. I. Conway, *Br. Dent. J.*, 2022, **233**, 780–786.
2 L. D. Punshon, M. R. Fabbrizi, B. Phoenix, S. Green and J. L. Parsons, *Cells*, 2024, **13**(24), 2065.
3 S. K. Sindhu and J. E. Bauman, *Oral Maxillofac. Surg. Clin. North Am.*, 2019, **31**, 145–154.
4 C. B. Dracham, A. Shankar and R. Madan, *Radiat. Oncol. J.*, 2018, **36**, 85–94.
5 M. Suzuki, I. Kato, T. Aihara, J. Hiratsuka, K. Yoshimura, M. Niimi, Y. Kimura, Y. Ariyoshi, S.-i. Haginomori, Y. Sakurai, Y. Kinashi, S.-i. Masunaga, M. Fukushima, K. Ono and A. Maruhashi, *J. Radiat. Res.*, 2013, **55**, 146–153.
6 Z. Zhang, Y. Chong, Y. Liu, J. Pan, C. Huang, Q. Sun, Z. Liu, X. Zhu, Y. Shao, C. Jin and T. Liu, *Cancers*, 2023, **15**, 4060.
7 W. H. Jin, C. Seldon, M. Butkus, W. Sauerwein and H. B. Giap, *Int. J. Part. Ther.*, 2022, **9**, 71–82.
8 E. Melia and J. L. Parsons, *Biosci. Rep.*, 2023, **43**(10), BSR20222586.
9 L. E. Farr, J. S. Robertson and E. Stickley, *Proc. Natl. Acad. Sci. U. S. A.*, 1954, **40**, 1087–1093.
10 M. A. Dymova, S. Y. Taskaev, V. A. Richter and E. V. Kuligina, *Cancer Commun.*, 2020, **40**, 406–421.
11 R. F. Barth, P. Mi and W. Yang, *Cancer Commun.*, 2018, **38**, 35.
12 P. Coghi, J. Li, N. S. Hosmane and Y. Zhu, *Med. Res. Rev.*, 2023, **43**, 1809–1830.
13 S. Wang, C. Blaha, R. Santos, T. Huynh, T. R. Hayes, D. R. Beckford-Vera, J. E. Blecha, A. S. Hong, M. Fogarty, T. A. Hope, D. R. Raleigh, D. M. Wilson, M. J. Evans, H. F. VanBrocklin, T. Ozawa and R. R. Flavell, *Mol. Pharmaceutics*, 2019, **16**, 3831–3841.
14 V. Ahire, N. Ahmadi Bidakhvidi, T. Boterberg, P. Chaudhary, F. Chevalier, N. Daems, W. Delbart, S. Baatout, C. M. Deroose, C. Fernandez-Palomo, N. A. P. Franken, U. S. Gaipl, L. Geenen, N. Heynickx, I. Koniarová, V. K. Selvaraj, H. Levillain, A. J. Michaelidesová, A. Montoro, A. L. Oei, S. Penninckx, J. Reindl, F. Rödel, P. Sminia, K. Tabury, K. Vermeulen, K. Viktorsson and A. Waked, in *Radiobiology Textbook*, ed. S. Baatout, Springer International Publishing, Cham, 2023, pp. 311–386.
15 T. Watanabe, Y. Sanada, Y. Hattori and M. Suzuki, *J. Radiat. Res.*, 2022, **64**, 91–98.
16 A. Farhat, F. Ahmad and H. Arafat, *Desalination*, 2013, **310**, 9–17.
17 C. D. B. Amaral, R. C. Machado, A. Virgilio, D. Schiavo, A. R. A. Nogueira and J. A. Nóbrega, *J. Anal. At. Spectrom.*, 2016, **31**, 1179–1184.
18 F. Yoshida, A. Matsumura, Y. Shibata, T. Yamamoto, H. Nakauchi, M. Okumura and T. Nose, *Cancer Lett.*, 2002, **187**, 135–141.
19 B. Verlinden, K. Van Hoecke, A. Aerts, N. Daems, A. Dobney, K. Janssens and T. Cardinaels, *J. Anal. At. Spectrom.*, 2021, **36**, 598–606.
20 M. Elinkmann, S. Reuter, M. Holtkamp, S. Heuckeroth, A. Köhrer, K. Kronenberg, M. Sperling, O. Rubner, C. D. Quarles, M. Hippler and U. Karst, *J. Anal. At. Spectrom.*, 2023, **38**, 2607–2618.
21 A. E. Olbrich, B. A. A. Stepec, N. Wurzler, E. C. Terol, A. Koerdt and B. Meermann, *Metallomics*, 2022, **14**, mfac083.

22 T. Nomizu, S. Kaneco, T. A. Tanaka, D. Ito, H. Kawaguchi and B. T. Vallee, *Anal. Chem.*, 1994, **66**, 3000–3004.
23 R. Álvarez-Fernández García, L. Gutiérrez Romero, J. Bettmer and M. Montes-Bayón, *Nanomaterials*, 2022, **13**(1), 12.
24 S. Y. Lim, Z. E. Low, R. P. W. Tan, Z. C. Lim, W. H. Ang, T. Kubota, M. Yamanaka, S. Pang, E. Simsek and S. F. Y. Li, *Metallomics*, 2022, **14**(12), mfac085.
25 M. Corte Rodríguez, R. Álvarez-Fernández García, E. Blanco, J. Bettmer and M. Montes-Bayón, *Anal. Chem.*, 2017, **89**, 11491–11497.
26 S. Meyer, A. López-Serrano, H. Mitze, N. Jakubowski and T. Schwerdtle, *Metallomics*, 2017, **10**, 73–76.
27 A. Galé, L. Hofmann, N. Lüdi, M. N. Hungerbühler, C. Kempf, J. T. Heverhagen, H. von Tengg-Kobligk, P. Broekmann and N. Ruprecht, *Int. J. Mol. Sci.*, 2021, **22**, 9468.
28 L. Konermann, Z. Liu, Y. Haidar, M. J. Willans and N. A. Bainbridge, *Anal. Chem.*, 2023, **95**, 13957–13966.
29 Q. Jin, T. Paunesku, B. Lai, S. C. Gleber, S. I. Chen, L. Finney, D. Vine, S. Vogt, G. Woloschak and C. Jacobsen, *J. Microsc.*, 2017, **265**, 81–93.
30 C. M. Nickson, P. Moori, R. J. Carter, C. P. Rubbi and J. L. Parsons, *Oncotarget*, 2017, **8**, 29963–29975.
31 C. Dordas and P. H. Brown, *Biol. Trace Elem. Res.*, 2001, **81**, 127–139.
32 C. Dordas and P. H. Brown, *J. Membr. Biol.*, 2000, **175**, 95–105.
33 C. E. Sims and N. L. Allbritton, *Lab Chip*, 2007, **7**, 423–440.
34 C. Y. Huang, Z. Y. Lai, T. J. Hsu, F. I. Chou, H. M. Liu and Y. J. Chuang, *J. Hepatocell. Carcinoma*, 2022, **9**, 1385–1401.
35 Y. C. Bai, Y. C. Hsai, Y. T. Lin, K. H. Chen, F. I. Chou, C. M. Yang and Y. J. Chuang, *Anticancer Res.*, 2017, **37**, 6347–6353.
36 J. Järvinen, H. Pulkkinen, J. Rautio and J. M. Timonen, *Pharmaceutics*, 2023, **15**(12), 2663.
37 P. Wongthai, K. Hagiwara, Y. Miyoshi, P. Wiriyasermkul, L. Wei, R. Ohgaki, I. Kato, K. Hamase, S. Nagamori and Y. Kanai, *Cancer Sci.*, 2015, **106**, 279–286.
38 M. Corte-Rodríguez, R. Álvarez-Fernández, P. García-Cancela, M. Montes-Bayón and J. Bettmer, *TrAC, Trends Anal. Chem.*, 2020, **132**, 116042.
39 Y. Cao, J. Feng, L. Tang, C. Yu, G. Mo and B. Deng, *Talanta*, 2020, **206**, 120174.

